

TID-4500, UC-35
Nuclear Explosions—
Peaceful Applications

Lawrence Radiation Laboratory
UNIVERSITY OF CALIFORNIA
LIVERMORE

UCRL-50563

**SCALED FREE-FIELD PARTICLE MOTIONS
FROM UNDERGROUND NUCLEAR EXPLOSIONS**

V. E. Wheeler

R. G. Preston

August 1, 1968

DISTRIBUTION STATEMENT A
Approved for Public Release
Distribution Unlimited

Reproduced From
Best Available Copy

20000908 119

DTIC QUALITY INSPECTED 4

Contents

Introduction	1
Parameters of Particle Motions and Scaling Rules	1
General Description of an Underground Nuclear Explosion	1
Free-Field Particle Motions	2
Scaled Free-Field Particle Motions	3
The Scaling Rules	3
Role of Explosion Medium	4
Curves of Scaled Particle Motions	6
Remarks	7
Acknowledgments	7
References	28

SCALED FREE-FIELD PARTICLE MOTIONS FROM UNDERGROUND NUCLEAR EXPLOSIONS

Introduction

In the past few years, a considerable amount of experimental information has been obtained from measurements of particle motions in stress waves from underground nuclear explosions. However, most of this information is in formats unsuitable for rapid, facile use by engineers and scientists interested in possible potential damage to test facilities from developmental testing of nuclear devices. Furthermore, with the exception of a single pioneering work by Perret¹ covering a study of particle motions from nuclear explosions in four varieties of rock, information from similar studies is scattered throughout the literature. This paper is an initial effort by the present authors to alleviate this situation. In the interest of expediency and in order to avoid classifying this paper, we have confined our present work to a survey of results from experiments by our co-workers and ourselves. In adhering to this principle of expediency, we have chosen to avoid summarizing results of studies in the hydrodynamic region.

Equations relating scaled free-field acceleration, a , peak radial stress, σ , velocity, u , and displacement δ , with scaled range, $R/W^{1/3}$ (R is the range, W the yield) are represented graphically in this report as follows:

$$aW^{1/3} = k_a (R/W^{1/3})^{-n_a}, \quad (1)$$

$$\sigma = k_\sigma (R/W^{1/3})^{-n_\sigma}, \quad (2)$$

$$u = k_u (R/W^{1/3})^{-n_u}, \quad (3)$$

$$\delta/W^{1/3} = k_\delta (R/W^{1/3})^{-n_\delta}, \quad (4)$$

where the k 's and n 's are characteristic of the parameter of motion and of the explosion medium. These equations, which have been derived from statistical fits to observations, are valid over limited scaled ranges. These ranges, although limited, are adequate, in most cases, for use in problems of potential damage to nuclear test facilities. Practice has fully demonstrated the utility to engineers and scientists of graphical representations for this application.

Parameters of Particle Motions and Scaling Rules

GENERAL DESCRIPTION OF AN UNDERGROUND NUCLEAR EXPLOSION

The sudden release of energy from detonation of a nuclear device in a

homogeneous, solid medium of infinite extent develops a spherically divergent shock wave, carrying with it energy from the explosion, and distributing this energy

by doing work on the surrounding medium. As the shock front moves radially from the shot point, it leaves behind, successively, vaporized material, melted material, crushed material, and cracked material. Eventually, the stress level in the shock front falls below the limiting stress to which the medium responds elastically. Beyond, energy is no longer irreversibly deposited in the medium, and the amplitude of the stress wave attenuates in accordance with classical theories of elasticity.

Stress in a radial direction from the center of the explosion in a solid medium predominates over stresses in tangential directions. Thus, the most potentially damaging effects of explosions are associated with the radial component of the stress wave.

Initially, the front of the shock wave from a nuclear explosion in a solid medium moves at a velocity considerably in excess of the sonic velocity characteristic of the medium. As the wave front moves radially outward, its strength and velocity decreases. The peak of the wave front lags more and more behind the leading edge. Eventually, the velocity of the leading edge falls to sonic velocity while trailing portions of the wave front fall to subsonic velocities. In the mean time, a stress wave with an amplitude corresponding, in an ideal medium, to the limiting stress which the medium will support elastically moves ahead of the main stress wave at sonic velocity. This stress wave, termed the elastic precursor, is fed continuously with energy from the trailing stress wave. The amplitude of the precursor is usually a small fraction of the amplitude of the main stress wave. Because of this, the pre-

cursor is of no importance to problems of damage from explosions in solid media.*

FREE-FIELD PARTICLE MOTIONS

As the stress wave from an explosion in a homogeneous solid moves outward from the center, it forces particles into motion. These particles attain maximum acceleration during the initial rise of stress; they attain maximum velocity at the time of peak stress; they attain maximum translation, or displacement, when stress in the oscillating wave train changes from positive to negative (i.e., crosses zero).† Measures of maximum radial components of particle motions in the first half-cycle of the stress wave from an explosion in a homogeneous medium of infinite extent are termed free-field particle acceleration, velocity, and displacement, respectively. Measures of one or more of these parameters of motion and/or of peak radial stress are important in estimating potential for damage from underground nuclear explosions. It is obvious that magnitudes of these motions are yield dependent. Magnitudes are also dependent upon physical

* A notable exception to this statement is that maximum acceleration from a nuclear explosion in unsaturated Nevada Test Site alluvium at appreciable distances from the explosion center is associated with the precursor to the main stress wave. (See notes to Figs. 1a and 1b.)

† More precisely, when "overpressure" in the stress wave initially falls to zero. Total pressure in the stress wave is the sum of stress generated by the explosion and ambient, or static, stress, usually overburden pressure. Except at low overpressures, or at great depths, ambient stress is a small fraction of maximum stress.

properties of the environment, to such an extent that knowledge of these properties, as will be discussed later, emerges as one of the most important factors to recognize in effects of underground nuclear explosions.

SCALED FREE-FIELD PARTICLE MOTIONS

The general expression relating free-field particle motions and peak radial stress with range is

$$f(m) = \phi_m(R, W), \quad (5)$$

in which $f(m)$ is the parameter of motion (or the radial stress) and $\phi_m(R, W)$ is a complex function of distance, R , from the center of the explosion of yield* W . Because, as mentioned above, magnitudes of motions are dependent upon properties of the explosion medium, the function $\phi(m)$ is also medium dependent. Scaling rules have been developed to relate these free-field particle motions and peak radial stresses from "tamped"† explosions in homogeneous media.

It may be shown by dimensional analysis that distances and times in the spherical stress wave from a point-source explosion in a solid medium scale with the cube root of the yield, or

$$f(m) = \phi'_m(R/W^{1/3}). \quad (6)$$

*Yield as used herein denotes energy released by the explosion. The unit of yield used is one kiloton of high-explosive equivalent.

†Tamped as used herein denotes closely coupled as contrasted with "decoupled." An explosion detonated in a large underground cavity is an example of a decoupled explosion. Work in this paper is limited to discussion of tamped underground nuclear explosions.

To state this generalization more exactly, if there are two explosions of yields W_1 and W_2 in the same medium, with free-field accelerations a_1 and a_2 , peak radial stresses of σ_1 and σ_2 , free-field velocities of u_1 and u_2 , and free-field displacements of δ_1 and δ_2 , all at distances R_1 and R_2 ,

$$a_1 W_1^{1/3} / a_2 W_2^{1/3} = \phi_a(R_1/W_1^{1/3}) / \phi_a(R_2/W_2^{1/3}), \quad (7)$$

$$\sigma_1 / \sigma_2 = \phi_\sigma(R_1/W_1^{1/3}) / \phi_\sigma(R_2/W_2^{1/3}), \quad (8)$$

$$u_1 / u_2 = \phi_u(R_1/W_1^{1/3}) / \phi_u(R_2/W_2^{1/3}), \quad (9)$$

$$(\delta_1 / W_1^{1/3}) / (\delta_2 / W_2^{1/3}) = \phi_\delta(R_1/W_1^{1/3}) / \phi_\delta(R_2/W_2^{1/3}). \quad (10)$$

In the above equations the quantity $R/W^{1/3}$ is termed scaled range, the quantity $aW^{1/3}$ is termed scaled free-field acceleration, and the quantity $\delta/W^{1/3}$ is termed scaled free-field displacement. Peak radial stress, free-field velocity, and scaled free-field acceleration and displacement are dependent only on the medium and the scaled range.

THE SCALING RULES

While Eqs. (7) through (10) are exact for a point-source explosion in a homogeneous medium of infinite extent, they do not indicate magnitudes or rates of attenuation, both of which depend on physical properties of the explosion environment contained in the function $\phi(R/W^{1/3})$. In order to evaluate this function, two approaches are available. One approach, illustrated by

Butkovitch's work² with a nuclear explosion in granite, involves theoretical calculations using pertinent physical properties of the medium. A second approach is to fit experimental observations empirically to equations of the form of Eq. (6). The latter approach has been adopted for this paper.*

Ample data from explosions in solid media have shown that scaled free-field particle motions may be fitted, over limited scaled ranges, to equations of the general form

$$f(m) = k(R/W^{1/3})^{-n} \quad (11)$$

where $f(m)$ is peak radial stress or scaled free-field particle motion, $(R/W^{1/3})$ is the scaled range, as before, and k and n are experimentally determined constants characteristic of the parameter of motion and of explosion environment. It is seen

*Theoretical calculations are of distinct value, particularly for explosions in media in which particle motions have not been measured. Also, theoretical calculations are particularly useful for deriving stress-wave characteristics close to the explosion center, where measurements are difficult or of doubtful validity. However, it should be noted that free-field acceleration in the stress wave cannot be calculated from theory with currently available techniques.

that this equation is simply a special form of Eq. (6), in which $\phi'_m(R/W^{1/3})$ is a complex function of scaled range applicable over the full scaled range rather than a limited scaled range. Work by Perret¹ with underground nuclear explosions has demonstrated that equations of the form of Eq. (11) are valid over stress levels adequate, for the most part, for use in problems associated with damaging effects of underground nuclear explosions. Equations of this form for individual parameters of free-field particle motions are given as Eqs. (1) through (4).

It should be noted that curves constructed on log-log coordinate paper from equations of the form of Eq. (11) are straight lines. In practice, observed free-field particle motions together with ranges are scaled by the cube root of the yield, and these observations are then fitted statistically to equations of the form of Eq. (11). While such equations are useful, graphical representations are clearly of greater utility to engineers and scientists concerned with possible damage from underground nuclear testing. In this paper, graphical representations are utilized. Also, in order to convey some concept of reliability of curves, observed scaled free-field particle motions are plotted in these representations.

Role of Explosion Medium

It was mentioned on page 3 that magnitudes of free-field particle motions, in addition to being dependent upon yield, are dependent upon physical properties of the explosion medium, or environment.

Perret's earlier work with nuclear explosions¹ showed that free-field

particle velocities from an underground nuclear explosion in granite were roughly an order of magnitude greater than those from an explosion in desert alluvium lying above the static water table. Peak radial stresses associated with these velocities are approximated by the product of the

free-field particle velocity and impedance (product of the density and compressional elastic wave velocity*) of the explosion medium. Since the impedance of granite is about five times that of dry alluvium, peak radial stresses from explosions in these two media show a larger disparity than free-field particle velocities. Qualitatively, explosions in high-impedance media are characterized by larger peak radial stresses, velocities, and accelerations than are those in low-impedance media.

Through circumstance, earth media in which the U.S. conducts its developmental nuclear testing are limited to two classifications of rocks: alluvium[†] and volcanic rocks, the latter deposited either as ash or flow. Variations in physical properties of these two materials, however, are substantial and require recognition if one is to select a scaling curve most closely approximating conditions in the stress wave from a nuclear explosion in a particular environment.

* More precisely, the velocity of propagation of the peak of the particle velocity and of the peak of the radial stress, each of which is in phase with the other. In the region of inelastic response of the medium, this velocity is smaller than the compressional elastic wave velocity. In the region of perfectly elastic response of a homogeneous medium, the two velocities are equal. Ratios of velocity of propagation of the peak of the particle velocity to the compressional elastic wave velocity are larger in inelastic stress waves from explosions in high-impedance media. Compressional elastic wave velocities, as used later in this paper, are, in all cases, those derived for large masses of in situ rocks, not necessarily the same as those found for laboratory specimens.

[†] Nevada Test Site (NTS) alluvium is a mixture of eroded products of volcanic deposits and Paleozoic rocks.

Density and compressional velocity, of course, help to characterize a medium. Degree of saturation is particularly significant, especially with alluvium. Thus, locating the explosion center below the water table, in most cases, significantly increases the relative coupling efficiency of an explosion. Or, the degree of "dry porosity" (i.e., percentage of voids unfilled by water) as used by Springer³ in his study of P-wave amplitudes from underground nuclear explosions, is reflected in relative coupling efficiencies. Media with large percentages of unfilled voids significantly decouple stress waves from explosions in these media. Other properties, such as chemical constitution, affect relative coupling efficiency. To date, U.S. experience with nuclear explosions in non-silicate rocks has been limited to explosions in bedded and dome salt.

Table I is a compilation of properties of the several explosion media in which the U.S. has measured particle motions. Most of this information is self-explanatory, but some clarification of figures in the fourth column is desirable. Since the usual quantities measured in the stress wave from an underground nuclear explosion are acceleration and velocity, peak radial stress must be calculated. It is the product of the density, free-field velocity, and the propagation velocity of the peak of the particle velocity. Figures in the fourth column are this latter velocity for each medium, derived from particle-motion measurements in the inelastic region. (However, lacking data, the present authors have estimated this velocity in some cases.) At large scaled ranges propagation velocity of the peak should approach compressional elastic wave

Table I. Properties of several rocks used as explosion media for underground nuclear testing.

Explosion medium	Density (g/cc)	Compressional elastic wave velocity at shot depth (ft/sec)	Propagation velocity of peak of radial particle velocity (ft/sec)	Ratio of stress to particle velocity ^a (bars/ft/sec)	Source of data
Unsaturated near-surface alluvium	1.5	2,700 ^b	1,500 to 1,800 ^b	2.1 to 2.5	—
Unsaturated low-impedance alluvium	1.6	5,570	3,500	5.21	c
Unsaturated high-impedance alluvium	2.0	7,200	4,850 ^d	9.02	e
Saturated alluvium	2.35 ^f	12,500 ^f	9,100 ^{b,d}	19.9	—
Unsaturated zeolitized tuff	1.95	7,900	6,000 ^b	10.9	—
Saturated zeolitized tuff	2.0 ^f	9,000 ^f	8,000 ^b	14.9	—
Saturated andesite	2.35	12,500	9,500 ^d	20.7	Reference 4
Unsaturated granite, SHOAL	2.6	17,800	13,600 ^b	32.9	Reference 5
Unsaturated granite, HARD HAT	2.69	18,100	13,800 ^b	34.5	Reference 1
Dome salt, SALMON	2.2	15,300	12,350	25.3	Reference 6

^aRatio of the peak radial stress to free-field particle velocity. This ratio is computed using the propagation velocity of peak velocity (i.e., figures in fourth column of this table). It is applicable for calculation of stress in the inelastic region.

^bEstimates by present authors.

^cClassified report by W. R. Perret of Sandia Laboratory.

^dThese velocities were derived (or estimated) from measurements in the stress wave vertically above the explosions. At these shallow depths, compressional velocities were smaller than those tabulated for shot depths. Other propagation velocities in the fourth column were derived from measurements at the horizon of the explosions.

^eClassified report by P. L. Randolph, R. G. Preston, and V. E. Wheeler of LRL.

^fUnpublished data from co-workers.

velocity, although experimental verification of this is lacking. Use of compressional elastic wave velocities in place of propagation velocities of peak to compute

peak radial stresses from free-field particle velocities in the elastic region is probably a better approximation to conditions in the stress wave.

Curves of Scaled Particle Motions

Table II is an index to eight figures (Figs. 1a and 1b through 7) in which scaling

curves are depicted for the three parameters of scaled free-field particle motions

Table II. Index to figures with scaling curves.

Explosion medium	Parameter of motion	Figure number	Explosion medium	Parameter of motion	Figure number
Unsaturated low-impedance alluvium	Acceleration	1a and 1b	Saturated andesite	Acceleration	4
	Velocity	2		Velocity	5
	Displacement	3		Displacement ^a	—
Unsaturated high-impedance alluvium	Acceleration	1a and 1b	Unsaturated granite	Acceleration	6
	Velocity	2		Velocity	7
	Displacement	3		Displacement	3
Unsaturated tuff	Acceleration	4	Dome salt	Acceleration	6
	Velocity	5		Velocity	7
	Displacement ^a	—		Displacement	3

^aData too poor to establish curve.

versus scaled range for underground nuclear explosions in six earth media. In each of the indexed figures, data from which curves were derived are plotted. Curves of each parameter of particle motion and of peak radial stress versus range for the several explosion media are

depicted in four composite figures (Figs. 3, 8, 9, and 10). From this latter set of figures the reader may easily perceive the important role of explosion medium as reflected in the wide range in magnitudes of stress-wave characteristics in the different media.

Remarks

Clearly, there is a need for more particle-motion measurements to be made at nuclear explosions in media differing substantially from those summarized in this paper. The best opportunities for studies of this type lie with the developing technology of underground engineering

with nuclear explosives. It does not appear, at this time, that developmental nuclear tests will be conducted in media differing substantially from the two broad classes of soils, alluvium and volcanic deposits, which so far have been used as explosion media for these tests.

Acknowledgments

We are particularly grateful to W.R. Perret of Sandia Laboratory, Albuquerque, for permission to use data published by him in classified reports and other data as yet un-

published by him. We are also grateful to A. Holzer and J.W. Hadley of LRL and to W.R. Perret, each of whom offered valuable suggestions during drafting of this report.

NOTES TO FIGS. 1a AND 1b

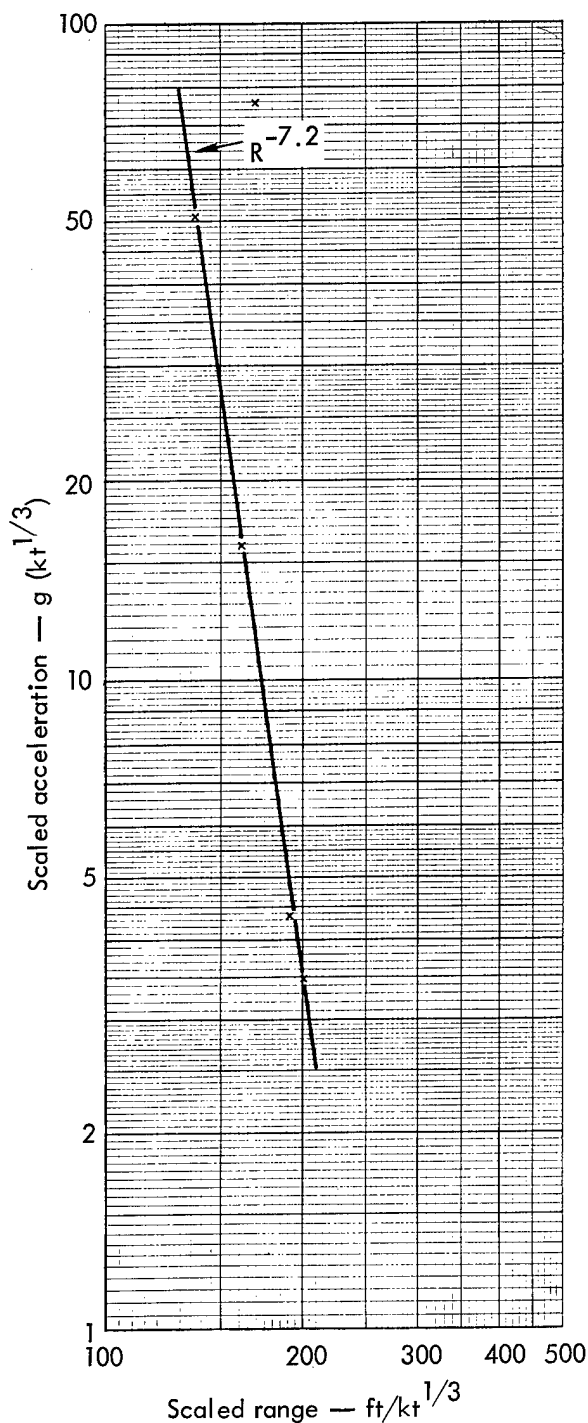


Fig. 1a. Scaled free-field acceleration versus scaled range for nuclear explosions in low- and high-impedance alluvium.

a. In dry alluvium at scaled ranges less than $175 \text{ ft/kt}^{1/3}$, peak accelerations are associated with the main stress wave and the normal scaling rules apply, with the data fitting an equation of the form

$$aW^{1/3} = k_a (R/W^{1/3})^{-n}$$

Thus Fig. 1a, in which scaled acceleration is plotted against scaled range, should be used for predicting maximum accelerations at scaled ranges less than $175 \text{ ft/kt}^{1/3}$ for moderate-yield shots normally fired in unsaturated alluvium. At scaled ranges greater than $175 \text{ ft/kt}^{1/3}$, maximum accelerations are associated with the elastic precursor. The data in this case fit an equation of the form

$$a = k_a (R/W^{1/3})^{-n}$$

Thus Fig. 1b, in which unscaled acceleration is plotted against scaled range, should be used for predicting maximum accelerations at scaled ranges greater than $175 \text{ ft/kt}^{1/3}$.

b. Free-field accelerations in dry alluvium were obtained from a classified report by R.G. Preston and V.E. Wheeler of LRL.

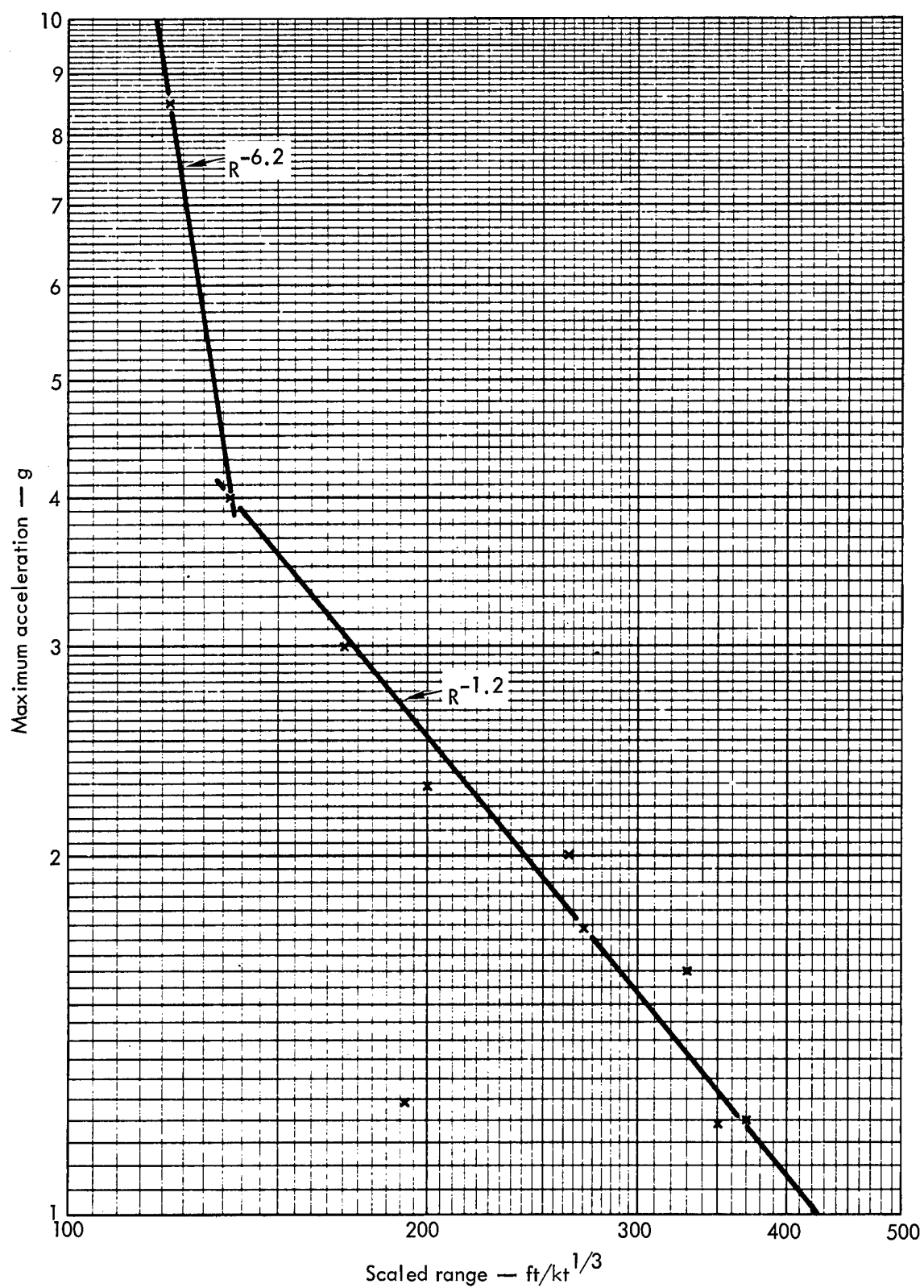


Fig. 1b. Maximum acceleration in precursor versus scaled range for nuclear explosions in low- and high-impedance alluvium.

NOTES TO FIGURE 2

a. Free-field velocities for nuclear explosions in unsaturated, low-impedance alluvium were obtained from two sources: a classified report by W. R. Perret of Sandia Laboratories (SL) and classified reports by R. G. Preston, V. E. Wheeler, and C. W. Olsen of LRL. Perret fitted his data to the curve illustrated; the LRL data are simply plotted in the figure.

b. Free-field velocities for nuclear explosions in unsaturated, high-impedance alluvium were obtained from two sources: a classified report by P. L. Randolph, R. G. Preston, and V. E. Wheeler of LRL and unpublished observations by W. R. Perret of SL. The curve is not a statistical fit to the data; instead, each limb of the curve is drawn parallel to the corresponding limb for low-impedance alluvium with an ordinate 1.5 times that of the latter.

LEGEND

- × SL data from low-impedance alluvium
- ◇ LRL data from low-impedance alluvium
- + SL data from high-impedance alluvium
- LRL data from high-impedance alluvium

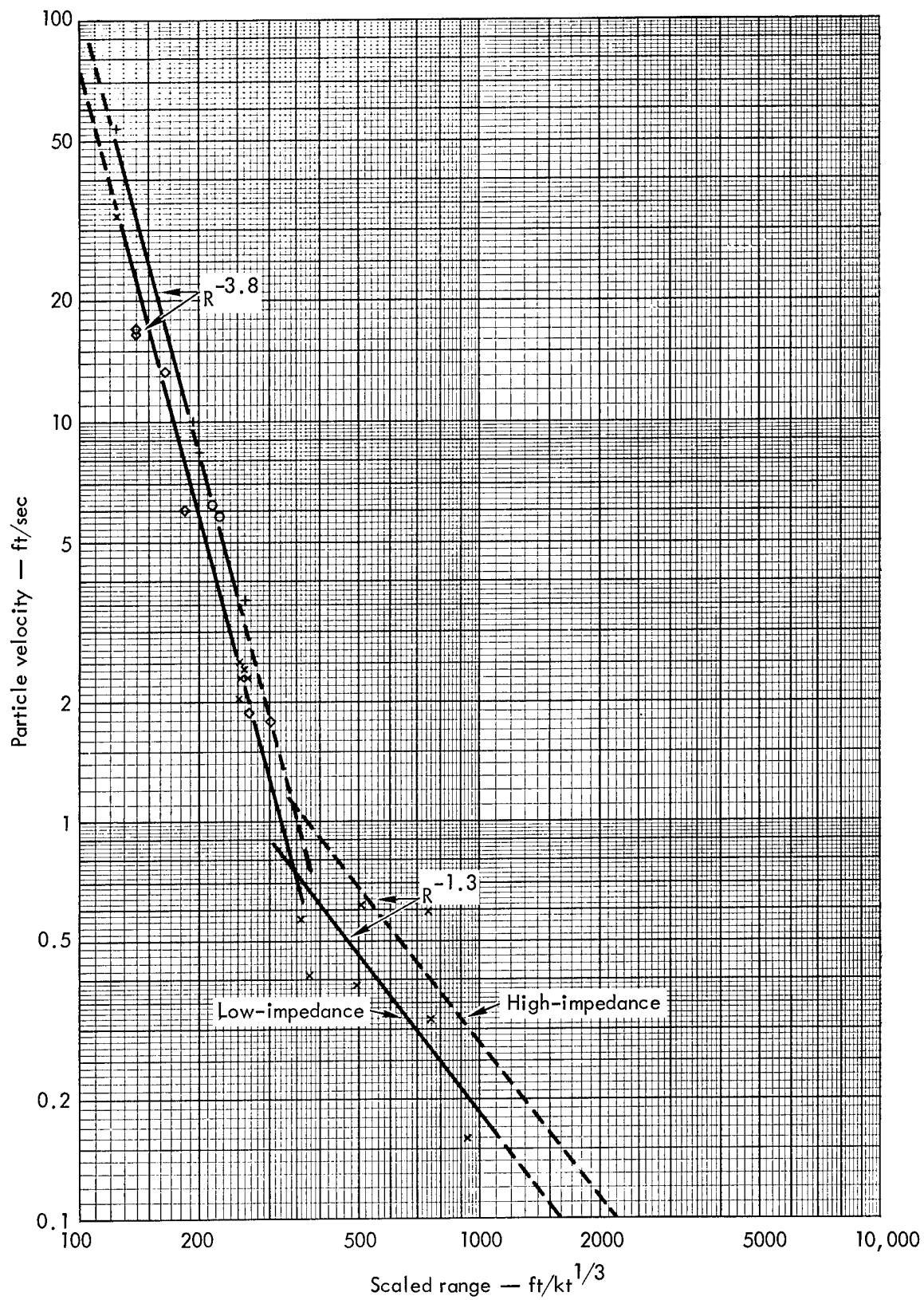


Fig. 2. Free-field particle velocity versus scaled range for nuclear explosions in low- and high-impedance unsaturated alluvium. Solid lines indicate regions covered by data.

NOTES TO FIGURE 3

a. Observed free-field displacements for nuclear explosions in both unsaturated tuff and saturated andesite were too scattered to establish curves for these two media.

b. No free-field displacement data are available for a nuclear explosion in unsaturated, high-impedance alluvium. The present authors recommend that a single curve, as depicted, be used for computing displacements for explosions in both low- and high-impedance unsaturated alluvium. It can be argued that, although free-field velocities are larger for explosions in high-impedance alluvium (see Fig. 2), both rise times to peak velocity and positive-phase durations of particle velocity are probably shorter, so that total impulse, i.e., free-field displacement, should be nearly equal for explosions in the two media.

c. Free-field displacements for nuclear explosions in unsaturated, low-impedance alluvium were obtained from two sources: a classified report by W.R. Perret of SL and a classified report by V.E. Wheeler and R.G. Preston of LRL. Perret derived the illustrated curve from his data.

d. Free-field displacements for a nuclear explosion in granite were obtained from work by Perret¹ at the 5.0-kt HARD HAT test. Perret derived the illustrated curve.

e. Free-field displacements for a nuclear explosion in dome salt were obtained from work by Perret⁶ at the 5.3-kt SALMON test. Perret derived the illustrated curve.

LEGEND

- × SL data from low-impedance alluvium
- ◇ LRL datum from low-impedance alluvium
- SL data from granite
- + SL data from dome salt

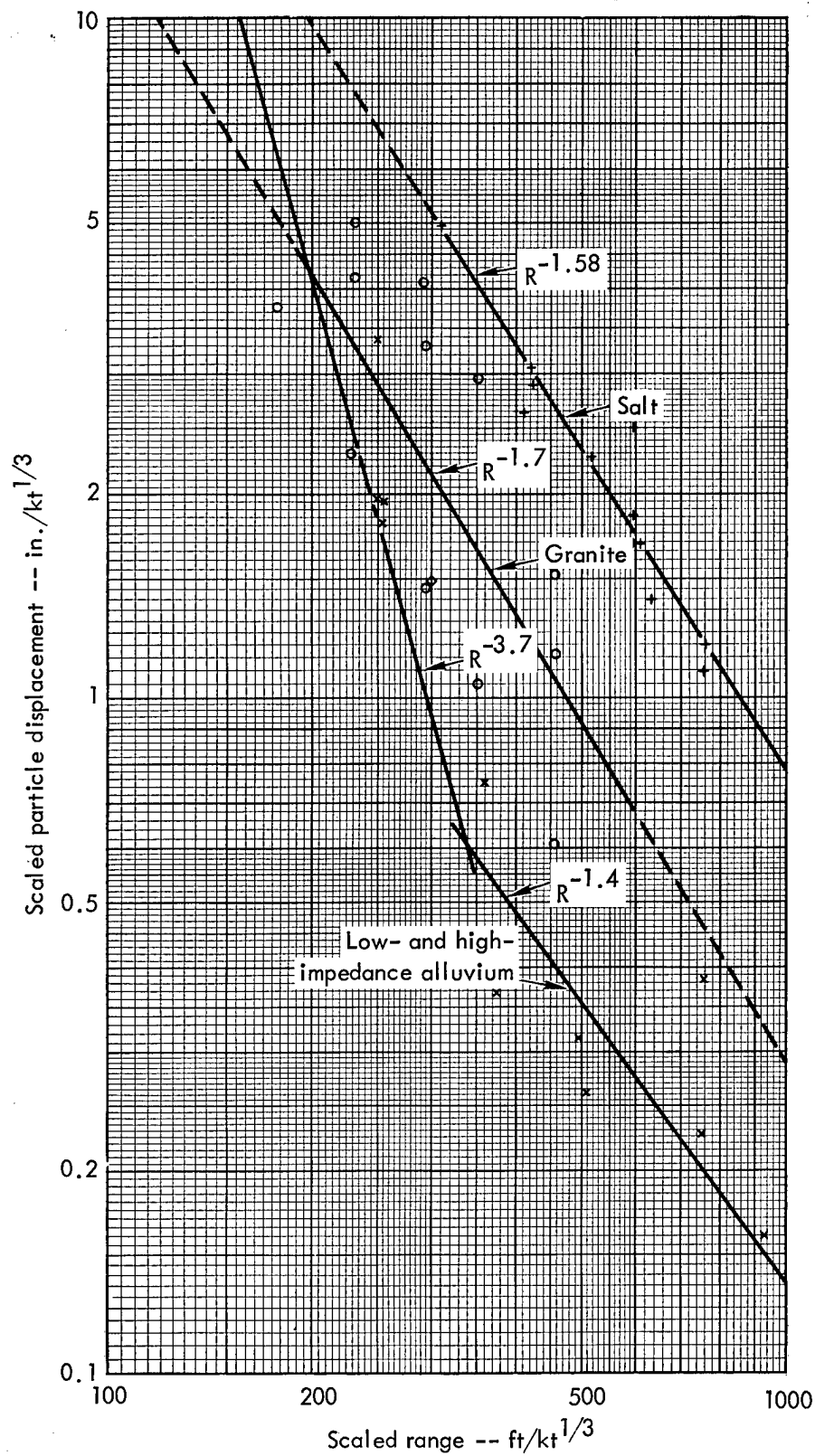


Fig. 3. Scaled free-field particle displacement versus scaled range for nuclear explosions in low- and high-impedance unsaturated alluvium, unsaturated granite, and salt. Solid lines indicate regions covered by data.

NOTES TO FIGURE 4

a. Free-field accelerations for a nuclear explosion in unsaturated tuff were obtained from work by Perret⁷ at the 1.7-kt RAINIER test. Perret derived the illustrated curve.

b. Free-field accelerations for a nuclear explosion in saturated andesite were obtained from work by Day and Murrell⁴ at the 80-kt LONG SHOT test. Day and Murrell derived the illustrated curve.

c. Fragmentary data from the January 19, 1968, underground nuclear test in Central Nevada, which was exploded in saturated alluvium similar in composition to NTS alluvium, indicate that the stress wave was very similar to that from an explosion in saturated andesite. Note the close similarity in densities and compressional velocities of these two media in Table I. The present authors recommend, subject to later revision, that curves for saturated andesite in this figure and in Figs. 5 and 10 be used for estimating free-field accelerations and velocities and peak radial stresses for underground nuclear explosions in saturated alluvium similar in composition to NTS alluvium.

LEGEND

- × SL data from unsaturated tuff
- WES data from saturated andesite

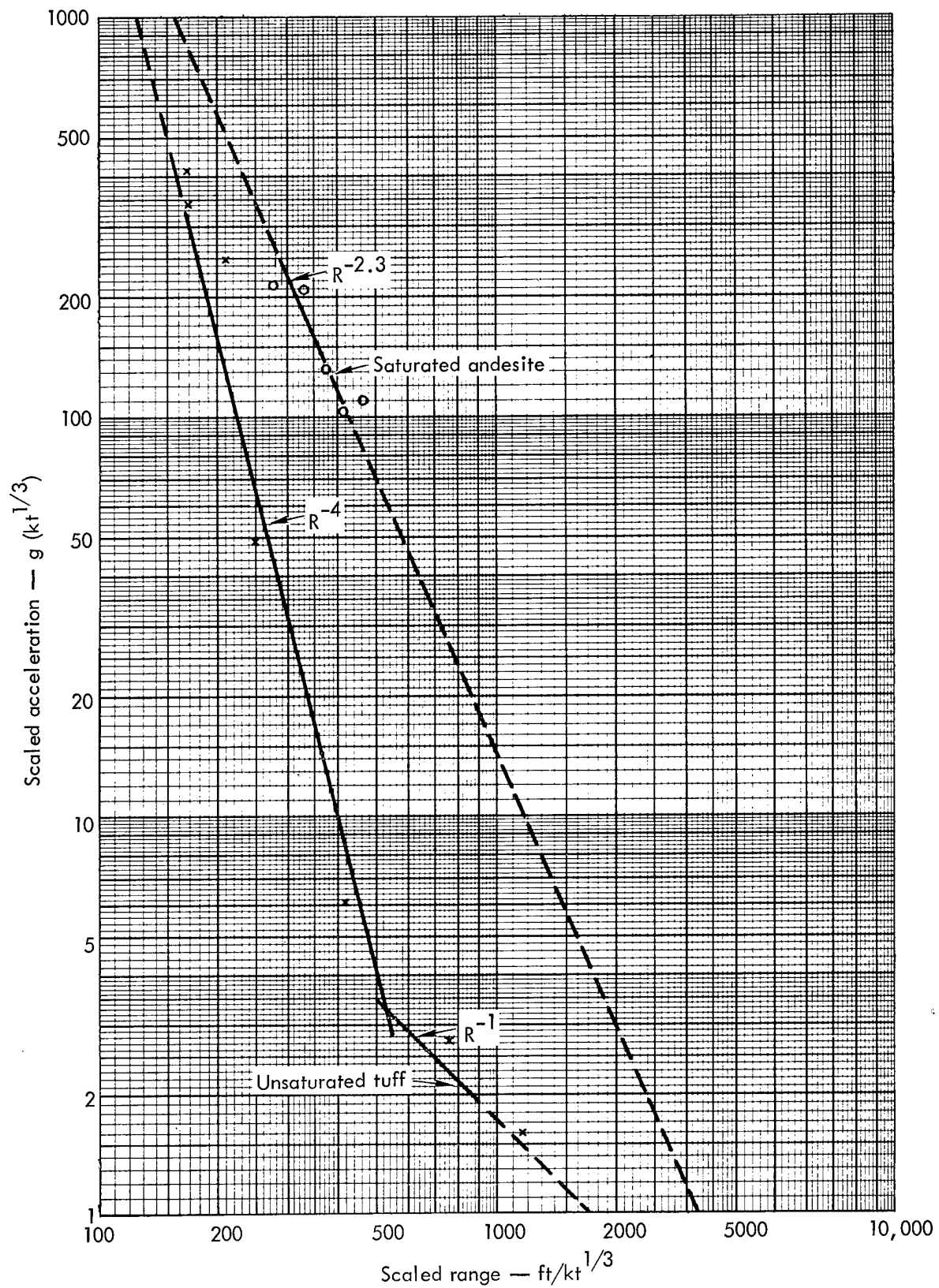


Fig. 4. Scaled free-field acceleration versus scaled range for nuclear explosions in unsaturated tuff and saturated andesite. Solid lines indicate regions covered by data.

NOTES TO FIGURE 5

a. Free-field velocities for a nuclear explosion in unsaturated tuff were obtained from work by Perret⁷ at the 1.7-kt RAINIER test. Perret derived the illustrated curve.

b. Free-field velocities for a nuclear explosion in saturated andesite were obtained from work by Day and Murrell⁴ at the 80-kt LONG SHOT test. The present authors derived the illustrated curve.

c. See Note c to Fig. 4.

LEGEND

- × SL data from unsaturated tuff
- WES data from saturated andesite

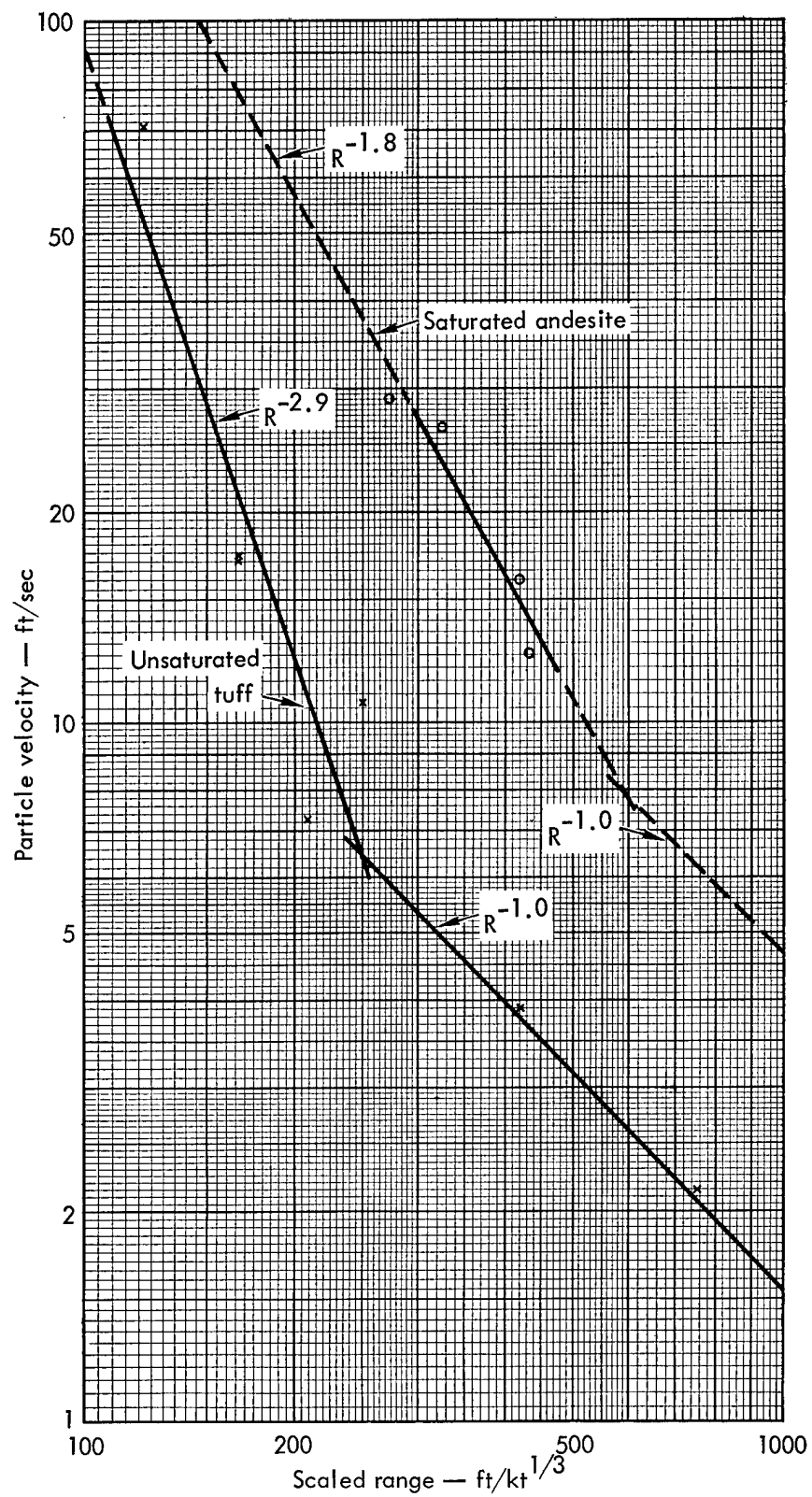


Fig. 5. Free-field particle velocity versus scaled range for nuclear explosions in unsaturated tuff and saturated andesite. Solid lines indicate regions covered by data.

NOTES TO FIGURE 6

a. Free-field accelerations for a nuclear explosion in unsaturated granite were obtained from work by Perret¹ at the 5.0-kt HARD HAT test. Perret derived the illustrated curve.

b. Free-field accelerations for a nuclear explosion in dome salt were obtained from work by Perret⁶ at the 5.3-kt SALMON test. Perret derived the illustrated curve.

LEGEND

- × SL data from granite
- SL data from dome salt

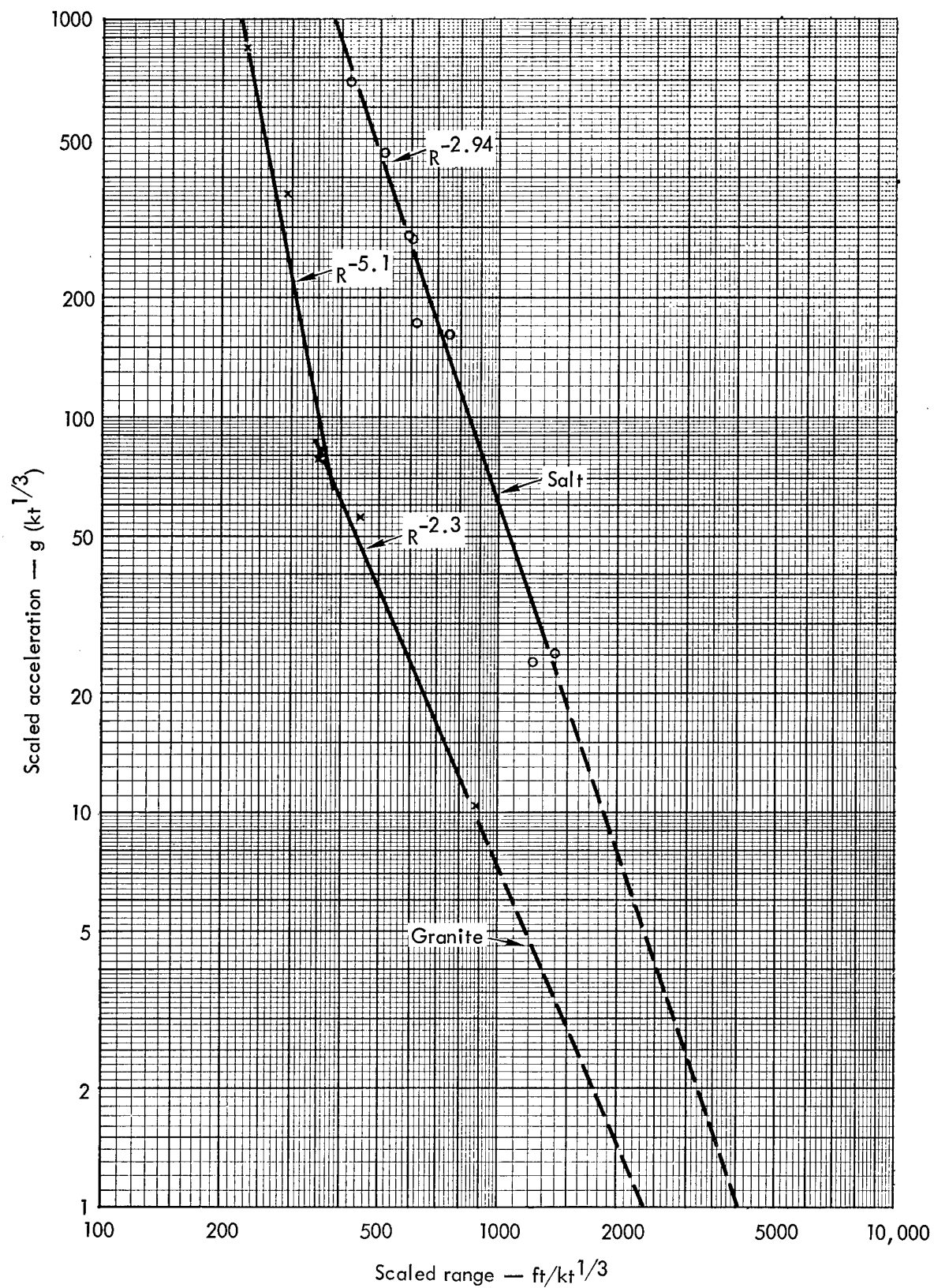


Fig. 6. Scaled free-field accelerations versus scaled range for nuclear explosions in unsaturated granite and salt. Solid lines indicate regions covered by data.

NOTES TO FIGURE 7

a. Free-field velocities for a nuclear explosion in unsaturated granite were obtained from work by Perret¹ at the 5.0-kt HARD HAT test. Perret derived the illustrated curve.

b. Free-field velocities for a nuclear explosion in dome salt were obtained from work by Perret⁶ at the 5.3-kt SALMON test. Perret derived the illustrated curve.

LEGEND

- × SL data from granite
- SL data from dome salt

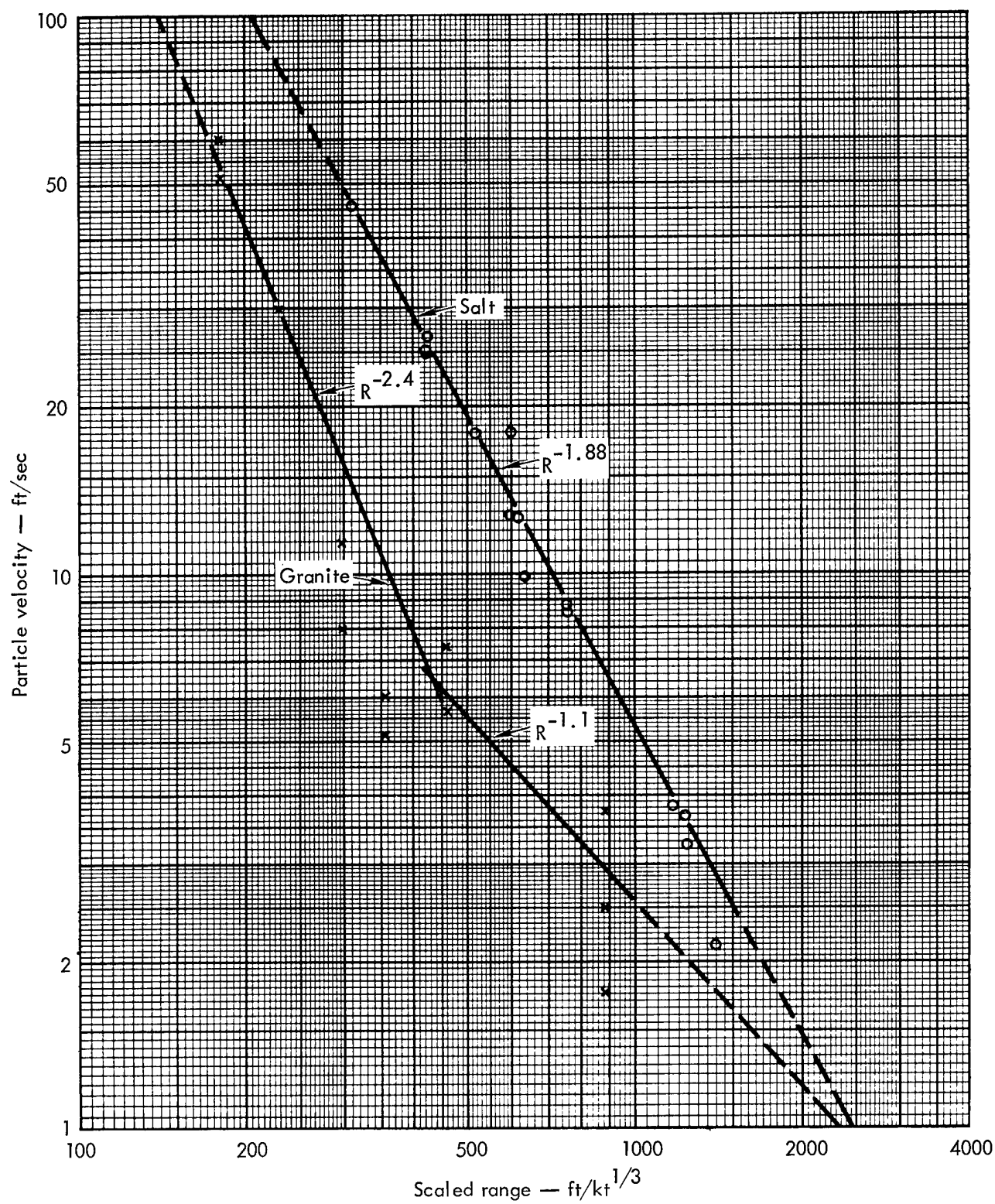


Fig. 7. Free-field particle velocity versus scaled range for nuclear explosions in unsaturated granite and salt. Solid lines indicate regions covered by data.

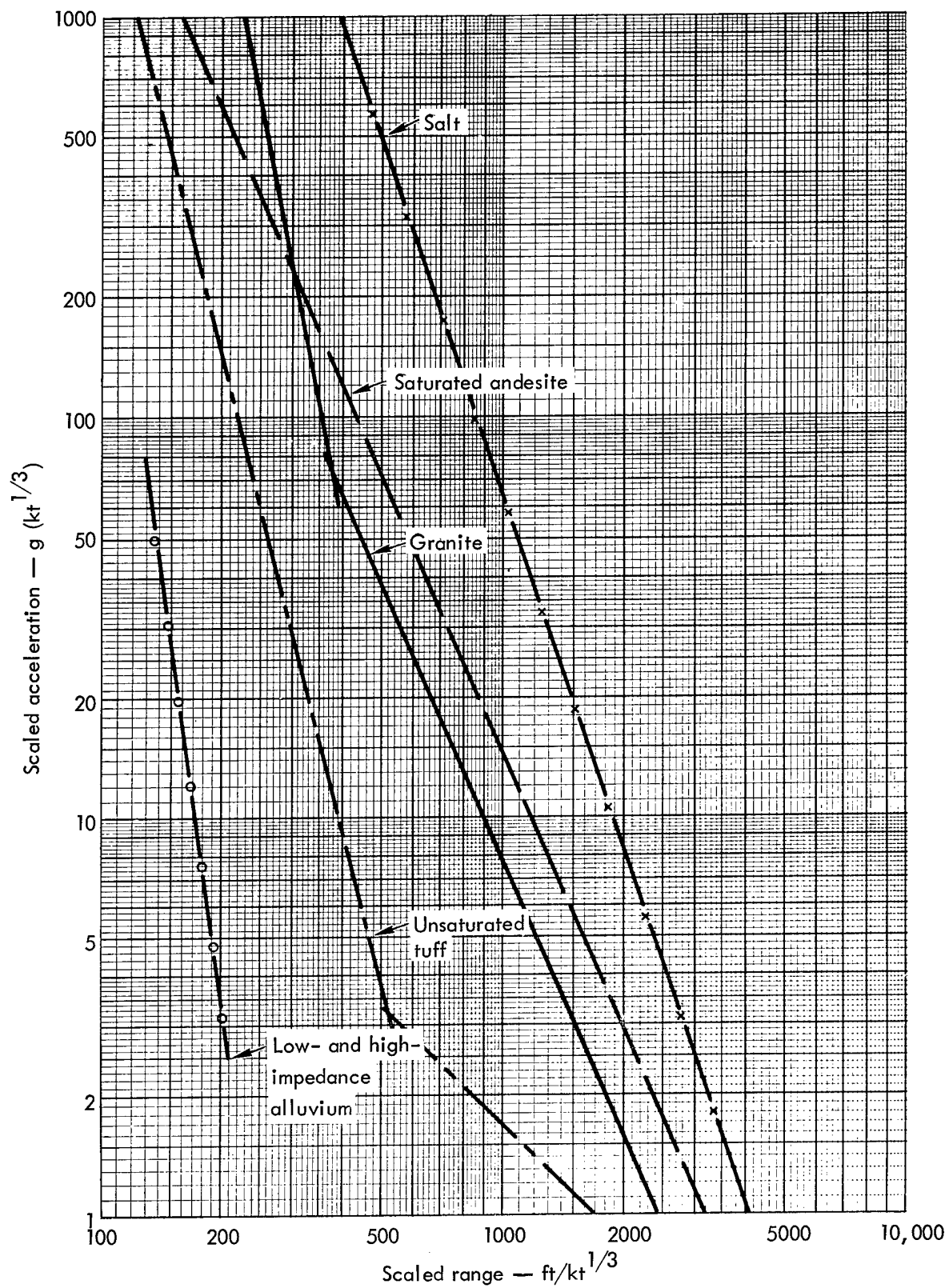


Fig. 8. Scaled free-field acceleration versus scaled range for nuclear explosions in six explosion media.

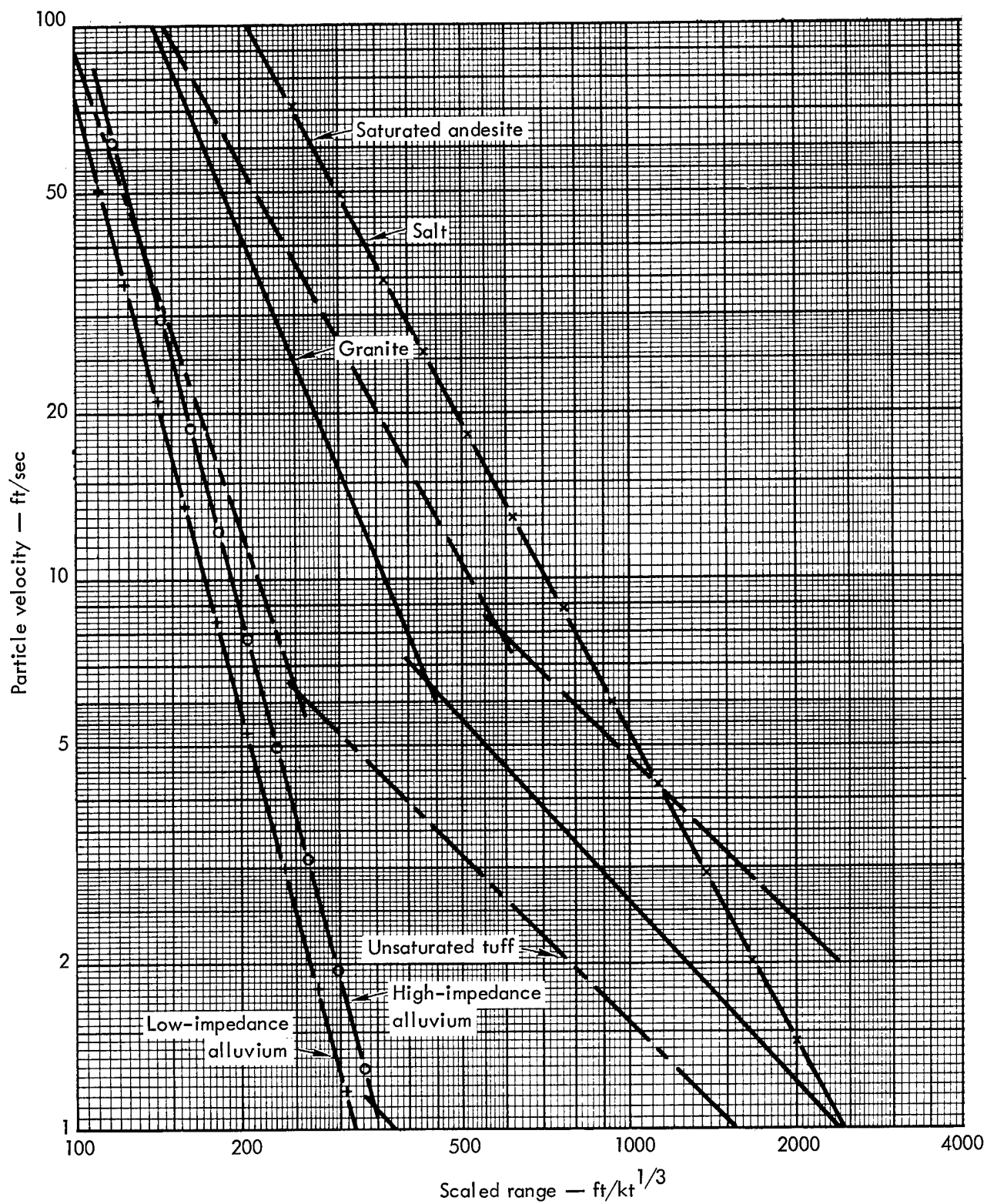


Fig. 9. Free-field particle velocity versus scaled range for nuclear explosions in six explosion media.

NOTES TO FIGURE 10

a. The upper limb of each two-limbed curve in this figure and the entire curve for salt is computed from the relation $\sigma - \sigma_0 = \rho uv$, where $\sigma - \sigma_0$ is the peak radial stress (σ_0 is the ambient pressure in front of the spherically expanding stress wave). ρ is the undisturbed density, u is the free-field velocity, and v is the velocity at which the peak of the stress wave propagates in the inelastic region. The lower limb of each curve is calculated as above except that v is set equal to the compressional velocity. (See "Role of Explosion Medium," page 4 .)

b. See Note c to Fig. 5.

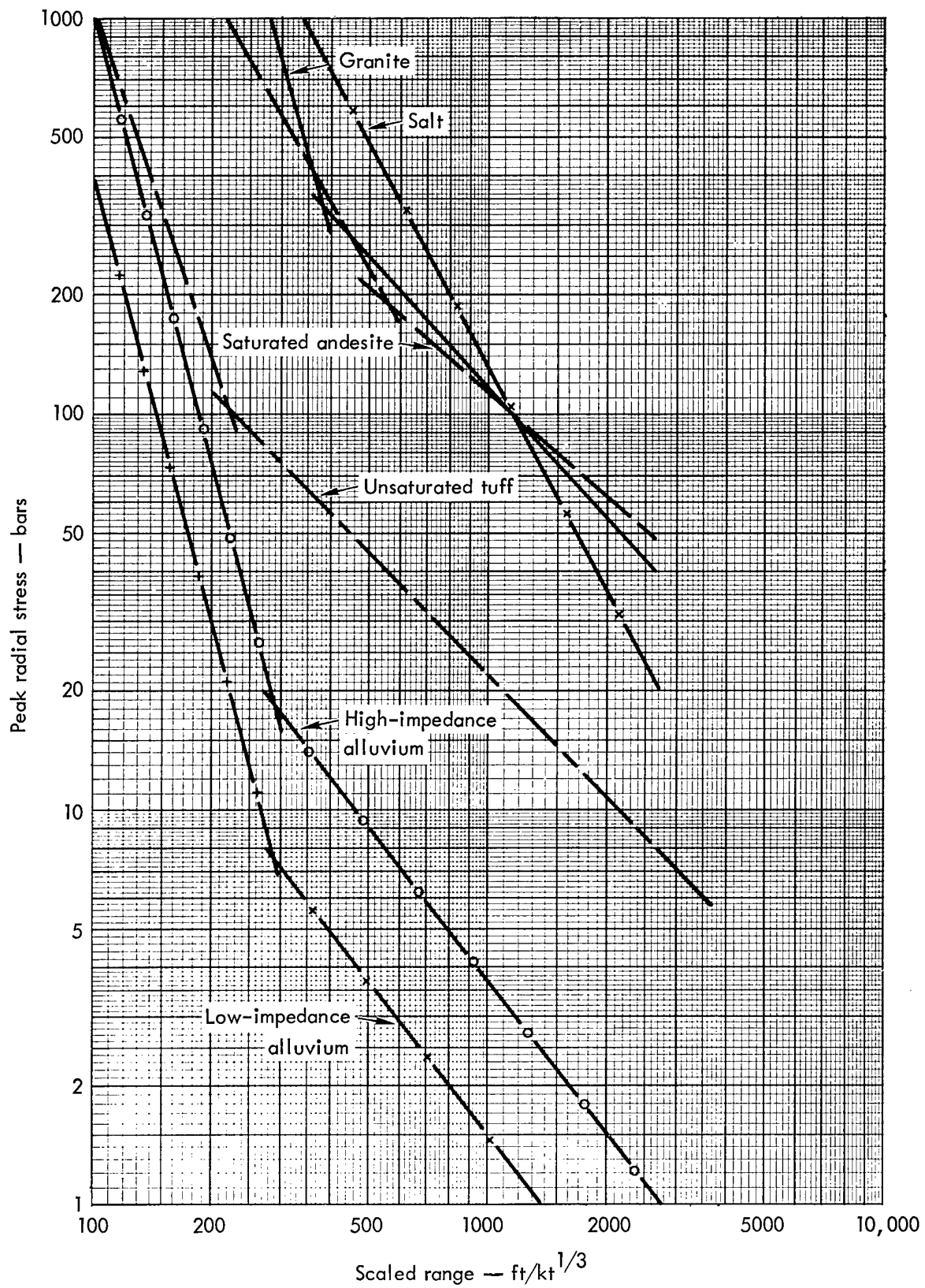


Fig. 10. Peak radial stress versus scaled radial range for nuclear explosions in six explosion media.

References

1. W. R. Perret, Free-Field Ground Motion Studies in Granite, Operation Nougat, Sandia Laboratory Report WT-1803, 19 April 1963 (Official Use Only).
2. T. R. Butkovich, "Calculation of the Shock Wave from an Underground Nuclear Explosion in Granite," J. Geophys. Res., 70, 885-892 (1965).
3. D. L. Springer, "P-Wave Coupling of Underground Nuclear Explosions," Bull. Seism. Soc. Am. 56, 861-876 (1966).
4. J. D. Day and D. W. Murrell, Ground and Water Shock Measurements, Waterways Experiment Station Report VUF-2701, 24 May 1967.
5. W. D. Weart, Free-Field Earth Motion and Spalling Measurements in Granite, Sandia Laboratory Report VUF-2001, February 1965.
6. W. R. Perret, Free-Field Particle Motion from a Nuclear Explosion in Salt, Part I, Sandia Laboratory Report VUF-3012, 21 June 1968.
7. W. R. Perret, Subsurface Motion from a Confined Underground Detonation, Part I, Operation Plumbbob, Sandia Laboratory Report WT-1529, May 1961.

Distribution

LRL Internal Distribution

Michael M. May

H. L. Reynolds

R. F. Herbst

G. C. Werth

G. H. Higgins

J. E. Carothers

V. N. Karpenko

J. N. Shearer

A. Holzer

L. S. Germain

J. W. Hadley

W. H. McMaster

D. C. Oakley

R. B. Petrie

A. B. Miller

P. A. House

C. E. Williams

P. E. Coyle

M. D. Nordyke

J. T. Cherry

J. S. Kahn

H. A. Tewes

C. W. Olsen

E. C. Jackson

B. C. Hudson

C. J. Sisemore

D. L. Springer

V. E. Wheeler

R. G. Preston

C. P. Benedix

D. L. Bernreuter

B. D. Faraudo

S. J. Spataro

R. C. Epps

T. Hamm, Jr.

R. A. Heckman

L. I. Starrh

J. R. Hearst

R. D. McArthur

Internal Distribution (Continued)

A. F. Clark	
L. F. Wouters	
A. L. Jorgensen	
D. M. Buchla	
N. D. Bailey	
J. K. Landauer	
G. P. D'Arcy	
TID Berkeley	
TID File	30

External Distribution

R. W. Newman	5
C. I. Browne, Jr.	
R. R. Brownlee	
C. G. Davis	
R. H. Campbell	
Los Alamos Scientific Laboratory	
Los Alamos, New Mexico	
B. F. Murphey	
C. D. Broyles	
M. L. Merritt	
W. R. Perret	3
W. D. Weart	
R. C. Bass	
G. E. Haensche	
B. C. Benjamin	2
A. D. Thornbrough	
Sandia Corporation	
Albuquerque, New Mexico	
H. F. Cooper, Jr.	5
Air Force Weapons Laboratory	
Kirtland AFB, New Mexico	
J. G. Lewis	5
Defense Atomic Support Agency	
Washington, D. C.	
B. Grote	5
Defense Atomic Support Agency	
Sandia Base	
Albuquerque, New Mexico	
D. A. Dicke	3
EG&G, Inc.	
Albuquerque, New Mexico	
J. D. Day	3
J. M. Polatty	
USAE Waterways Experiment Station	
Vicksburg, Mississippi	
F. M. Sauer	3
Stanford Research Institute	
Menlo Park, California	
R. E. Miller	5
U. S. Atomic Energy Commission	
Las Vegas, Nevada	

External Distribution (Continued)

R. R. Gunney Holmes and Narver, Inc. Las Vegas, Nevada	2
B. C. Hughes Nuclear Cratering Group Livermore, California	5
H. M. Puckett Defense Atomic Support Agency Livermore, California	
K. W. King Environmental Science Services Administration Coast and Geodetic Survey Las Vegas, Nevada	
R. F. Beers Environmental Research Corporation Alexandria, Virginia	
C. S. Clark P. Stewart EG&G, Inc. Goleta, California	
C. R. Runnion EG&G, Inc. Las Vegas, Nevada	
TID-4500 Distribution, UC-35, Nuclear Explosions — Peaceful Applications 255	

LEGAL NOTICE

This report was prepared as an account of Government sponsored work. Neither the United States, nor the Commission, nor any person acting on behalf of the Commission:

A. Makes any warranty or representation, expressed or implied, with respect to the accuracy, completeness, or usefulness of the information contained in this report, or that the use of any information, apparatus, method, or process disclosed in this report may not infringe privately owned rights; or

B. Assumes any liabilities with respect to the use of, or for damages resulting from the use of any information, apparatus, method or process disclosed in this report.

As used in the above, "person acting on behalf of the Commission" includes any employee or contractor of the Commission, or employee of such contractor, to the extent that such employee or contractor of the Commission, or employee of such contractor prepares, disseminates, or provides access to, any information pursuant to his employment or contract with the Commission, or his employment with such contractor.

Printed in USA. Available from the Clearinghouse for Federal
Scientific and Technical Information, National Bureau of Standards,
U. S. Department of Commerce, Springfield, Virginia 22151
Price: Printed Copy \$3.00; Microfiche \$0.65.